

A Fault Current Limiter Circuit to Improve Transient Stability in Power System

Saumen Dhara¹, Alok Kumar Shrivastav², Pradip Kumar Sadhu³, Ankur Ganguly⁴

¹Saroj Mohan Institute of Technology, West Bengal-712512, India

^{2,4}Techno India Batanagar, West Bengal-700141, India

³Indian School of Mines, Dhanbad-826004, India

Article Info

Article history:

Received Nov 12, 2015

Revised Mar 19, 2016

Accepted Apr 20, 2016

Keyword:

Fault protection

Superconducting fault current limiter (SFCL)

Transient stability

Transmission systems

ABSTRACT

Short circuit current limitation in distribution system utilities can be an operational approach to improve power quality, since the estimated voltage sag amplitude during faults may be intensely reduced. The application of superconducting fault current limiter (SFCL) is projected here to limit the fault current that occurs in power system. SFCL utilizes superconductors to instantaneously decrease the unanticipated electrical surges that happen on utility distribution and power transmission networks. SFCL considerably decrease the economic burden on the utilities by reducing the wear on circuit breakers and protecting other expensive equipment. The designed SFCL model is used for determining an impedance level of SFCL according to the fault current limitation necessities of different types of the smart grid system. The representation of this paper about to see the optimum resistive value of SFCL for enhancing the transient stability of a power system. The assessment of optimal resistive value of the SFCL connected in series in a transmission line with a conductor throughout a short circuit fault is consistently determined by applying the equal-area criterion supported by power-angle curves. A Simulink based primary model is developed and additionally the simulation results for the projected model are achieved by using MATLAB.

*Copyright © 2016 Institute of Advanced Engineering and Science.
All rights reserved.*

Corresponding Author:

Alok Kumar Shrivastav,

Department of Electrical Engineering,

Techno India Batanagar (A Unit of Techno India Group),

B7-360 / New, Ward No. 30, Putkhali, Maheshtala, Kolkata-700141 West Bengal, India.

Email: alok5497@gmail.com

1. INTRODUCTION

The suitability of electric power to customer devices is suggested by the power quality. The synchronization of the voltage, frequency and phase permits electrical systems to perform in their proposed manner while not vital loss of performance or its life. Power quality is an important matter that is turning into gradually increasing with necessary to electricity consumers in any respect of all stages of usage. Suitable sensitive power electronic equipment and non-linear loads are extensively utilized in industrial, commercial and domestic applications resulting in distortion in voltage and current waveforms. Each electrical utilities and end users of electrical power have become gradually increasing and that are involved concerning the quality of electrical power. For the protection purpose of excessive fault current in power systems, conventional protection devices are installed, specifically at the high voltage substation area. The tripping of circuit breakers depends on overcurrent protection relay that has a response time delay that allows initial two or three fault current cycle to pass before getting activated [1]. The superconducting fault current limiter (SFCL) is innovative electric equipment, which has the capability to reduce fault current level within the first cycle of fault current [2]. The first-cycle suppression of fault current by a SFCL results in an

increased transient stability of the power system carrying higher power with greater stability [3]. As the scale of power systems is increasing day by day with distributed generation [6], [7] connected to a grid, high-level fault currents might be caused during a contingency. Recently, many devices such as split bus bars, transformers with higher impedance, and fuses have been used in industry to reduce the peak value of fault currents. However, the use of these devices has limits, in that they can damage the reliability of the power system or increase power loss [8]. A fault current limiter based on a high temperature superconductor can be an alternative to replace the aforementioned conventional devices. In other way we can say, the superconducting fault current limiter (SFCL) can improve the transient stability of the power system by suppressing the level of fault currents in a fast and effective manner. In the past two decades, many studies on the application of high-temperature SFCLs to electric power systems have been carried out [9]–[11], and various types of SFCLs have been designed until now. Moreover, the SFCL with good performance is currently being made in industry. The next step is to apply the developed SFCL to power systems for practical use. For this goal, the following three important factors must be considered:

- i. Optimal place to install the SFCL.
- ii. Optimal resistive value of the SFCL connected in series with a transmission line during a short-circuit fault.
- iii. Potential protection-coordination problem with other existing protective devices such as a recloser and a circuit breaker.

This paper focuses on factor (ii) for the resistive-type SFCL, which is useful to improve the reliability of the system [12], with the transient stability study based on the equal-area criterion [13]. In addition, the performances of the proposed SFCL to reduce the level of fault currents are evaluated with simulation MATLAB software. Finally, this paper makes a new contribution by determining the optimal resistive value of the SFCL based on the systematic approach by the equal-area criterion when compared to the previous work [14] by introducing the simple concept of SFCL with its equivalent circuit. Finally, the simulation results to show the effectiveness of the proposed SFCL with the appropriate parameter.

2. POWER SYSTEM MODEL

A comprehensive model of power network including generation, transmission, and distribution system is implemented in it.

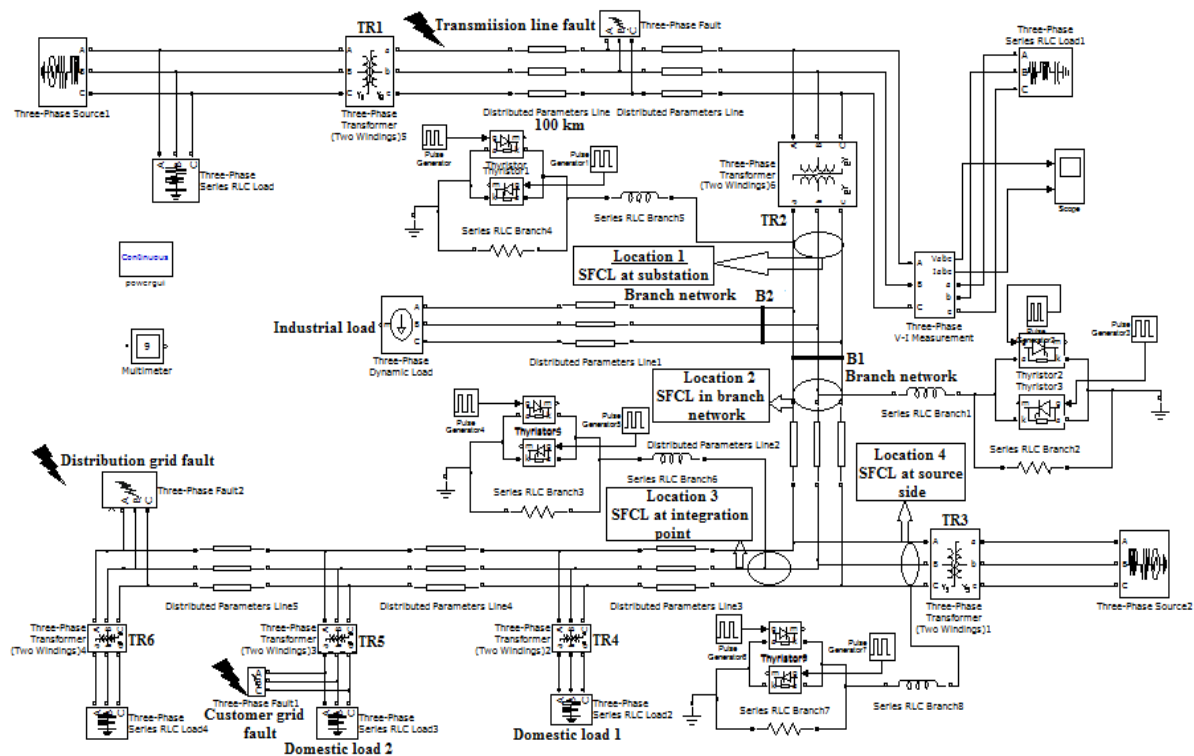


Figure 1. Power system model designed in Simulink

Hence, three-phase source with the distribution network is designed for implementing the newly developed micro grid model. Figure 1 shows the power system model designed in Simulink. The power system is composed of two 25 KV (Phase-to-phase RMS voltage) 3-phase source connected with 200 km long 154 kV distributed-parameters transmission line through a step-up transformer TR1. Here the voltage is stepped down to 22.9 kV from 154 kV, at the substation (TR2). In this system the high power separate distribution branch networks are supplying industrial load (6 MW) and low power domestic loads (1 MW each). The three-phase voltage source is directly coupled with the branch network (B1) through transformer TR3 and is providing power to the domestic loads. The domestic load is being rated with 3 MVA, out of which 2.7 MVA is being provided by the three-phase source, during the time of fault. In the diagram of Figure, three kinds of fault points are marked as Fault 1, Fault 2 and Fault 3 are indicated as three phase line-line faults in distribution grid, customer grid and transmission line respectively. Four prospective locations for SFCL installation are marked as Location 1 (Substation/Three phase source), Location 2 (Branch Network), Locations 3 (Integration point with the grid) and Location 4 (Three-phase source at the end). Usually, conventional fault current protection devices in the transmission system are located in Location 1 and Location 2. The output current of three phase source (the output of TR3 in Figure 1) for various SFCL locations have been measured and analysed for determining the optimum location of SFCL in a micro grid.

3. RESISTIVE SFCL MODEL

The three phase resistive type SFCL was modelled considering four fundamental parameters of a resistive type SFCL. The parameters and their selected values are: 1) transition or response time = 2 m sec, 2) minimum impedance = 0.01 ohms and maximum impedance = 20 ohms, 3) triggering current = 550A and 4) recovery time=10 msec. Its working voltage is 22.9 kV.

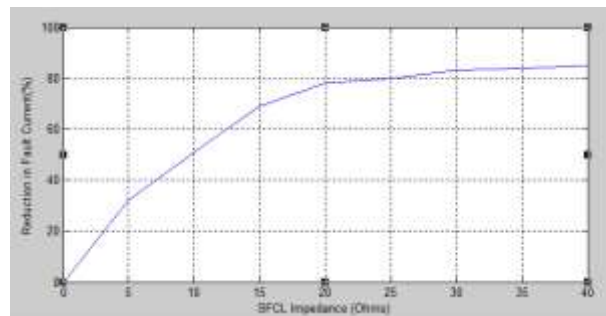


Figure 2. SFCL impedance and reduction in fault current

Figure 3 shows the result of verification test of SFCL model conducted on power network model depicted in Figure 1. SFCL has been located at substation (Location 1) and for a distribution grid fault (Fault 1), various SFCL impedance values versus its fault current reduction operation has been plotted. Maximum fault current (No SFCL case) is 7500 A at 22.9 kV for this arrangement.

4. STABILITY ANALYSIS IN A POWER SYSTEM WITH SFCL

The simple structure of a resistive (non-inductive winding) SFCL unit is shown in Figure 3. A unit consists of the stabilizer resistance of the n^{th} unit $R_{ns}(t)$, the superconductor resistance of the n^{th} unit $R_{nc}(t)$, which is connected with $R_{ns}(t)$ in parallel and the coil inductance of the n^{th} unit L_n . The subscript n denotes the number of connected units.

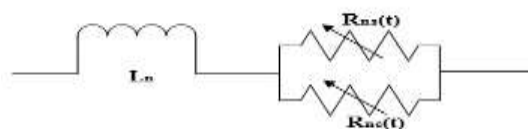


Figure 3. Simple structure of a resistive SFCL unit

The standard values of $R_{nc}(t)$ and $R_{ns}(t)$ of the SFCL are generally zero during a usual steady-state situation. The importance of total resistance R_{SFCL} of the SFCL throughout a fault is determined by the entire quantity of units in Figure 4, which are coupled in series. The value of L_n is estimated by the turns of coils. This value has to be as less as probable due to inductance causes ac power loss in usual state. Thus, the related equation for R_{SFCL} is stated by (1) to explain its quenching and recovery features.

$$R_{SFCL}(t) = \begin{cases} 0, & (t_0 > t) \\ R_m \left[1 - \exp\left(-\frac{t-t_0}{T_{SC}}\right) \right]^{\frac{1}{2}}, & (t_0 \leq t < t_1) \\ a_1(t - t_1) + b_1, & (t_1 \leq t < t_2) \\ a_1(t - t_2) + b_2, & (t_2 \leq t) \end{cases} \quad (1)$$

where R_m is the maximum resistance of the SFCL in the quenching state, T_{SC} is the time constant of the SFCL during transition from the superconducting state to the normal state. Furthermore, t_0 is the time to start the quenching. Finally, t_1 and t_2 are the first and second recovery times, respectively. A synchronous machine and a transmission system connected to an infinite bus represented as in Figure 4 as a simple power system. During a steady state, condition the value of R_{SFCL} is zero as indicated before. When a three-phase short circuit or the other grounding faults is occurred and when an infinite bus is operated with a fault resistance of R_f , the SFCL linked in series to the transmission line functions instantly with an exact resistive value of R_{SFCL} , as indicated in Figure 4.

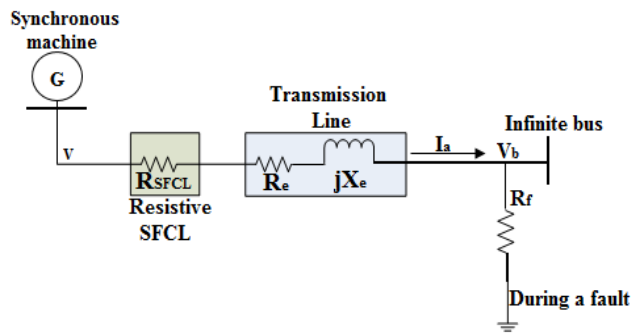


Figure 4. SMIB system with a resistive SFCL

$$P = \frac{|E_1||V_1|}{X_{d1}} \sin\beta + |V_1|^2 \frac{X'_{d1} \cdot X'_{q1}}{2X_{d1}X_{q1}} \sin 2\beta \quad (2)$$

In the above equation, E_1 is the no-load generated electromotive force and V_1 is the machine terminal voltage. Also, X_{d1} and X_{q1} are the direct and quadrature axis reactances of the synchronous generator, respectively. To analyze the effect of R_{SFCL} on the power system during a fault, the phasor diagram with reference of V in Figure 5(a) is changed to the phasor diagram in Figure 5(b) with reference of the infinite-bus voltage. In addition, the associated equations are expressed as

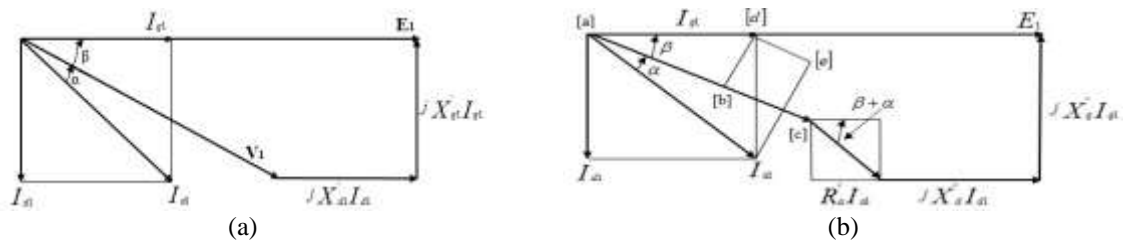


Figure 5. Phasor diagram of the SMIB system

$$\mathbf{R}_a'' = \mathbf{R}_{a1} + \mathbf{R}_{e1} + \mathbf{R}_{SFCL} + \mathbf{R}_{f1} \quad (3)$$

$$\begin{aligned} \mathbf{X}_d'' &= \mathbf{X}_{d1}'' + \mathbf{X}_{q1}'' \\ \mathbf{X}_q'' &= \mathbf{X}_{q1}'' + \mathbf{X}_{e1}'' \end{aligned} \quad (4)$$

where R_e the armature resistance of the synchronous machine is, the transmission-line resistance, and X_e is the transmission-line reactance. Then, the power-angle equation for the analysis of R_{SFCL} can be derived as follows. First, the real power P is given by

$$P = |\mathbf{V}_{bl}| |\mathbf{I}_{a1}| \cos \alpha = |\mathbf{V}_{bl}| (\mathbf{I}_{q1} \cos \beta + \mathbf{I}_{d1} \sin \beta) \quad (5)$$

where $|\mathbf{I}_{a1}| \cos \alpha$ is the distance between points [a] and [c] in Figure 5 (b), which can be represented as The distance between intermediate points [a] and [c] and may be represented as

$$|\mathbf{I}_{a1}| \cos \alpha = \bar{ac} = \bar{ab} + \bar{bc} = \bar{ab} + \bar{de} = \mathbf{I}_{q1} \cos \beta + \mathbf{I}_{d1} \sin \beta \quad (6)$$

The currents obtained I_{d1} and I_{q1} from d-q axis, are expressed as

$$\begin{aligned} |\mathbf{V}_{bl}| \cos \beta &= |\mathbf{E}_1| - \mathbf{X}_d'' \mathbf{I}_{d1} - \mathbf{R}_a'' \mathbf{I}_{a1} \cos(\beta + \alpha) \\ |\mathbf{V}_{bl}| \sin \beta &= \mathbf{X}_q'' \mathbf{I}_{q1} - \mathbf{R}_a'' \mathbf{I}_{a1} \sin(\beta + \alpha) \end{aligned} \quad (7)$$

$$\begin{aligned} \mathbf{I}_{d1} &= \frac{|\mathbf{E}_1| - |\mathbf{V}_{bl}| \cos \beta - \mathbf{R}_a'' \mathbf{I}_{a1} \cos(\beta + \alpha)}{\mathbf{X}_d''} \\ &= \mathbf{I}_{a1} \sin(\beta + \alpha) \\ \mathbf{I}_{q1} &= \frac{|\mathbf{V}_{bl}| \sin \beta + \mathbf{R}_a'' \mathbf{I}_{a1} \sin(\beta + \alpha)}{\mathbf{X}_q''} \\ &= \mathbf{I}_{a1} \cos(\beta + \alpha) \end{aligned} \quad (8)$$

Finally, the currents I_{d1} and I_{q1} are expressed as

$$\mathbf{I}_{d1} = \frac{\mathbf{X}_q'' (|\mathbf{E}_1| - |\mathbf{V}_{bl}| \cos \beta) - \mathbf{R}_a'' |\mathbf{V}_{bl}| \sin \beta}{\mathbf{R}_a''^2 + \mathbf{X}_d'' \mathbf{X}_q''} \quad (9)$$

$$\mathbf{I}_{q1} = \frac{\mathbf{R}_a'' (|\mathbf{E}_1| - |\mathbf{V}_{bl}| \cos \beta) + \mathbf{X}_d'' |\mathbf{V}_{bl}| \sin \beta}{\mathbf{R}_a''^2 + \mathbf{X}_d'' \mathbf{X}_q''} \quad (10)$$

The new power angle equation can be established as follows, expressed in equation no (11) by putting the values of currents I_{d1} and I_{q1} from equations (9) and (10) in the equation no (5).

$$P = \frac{|\mathbf{V}_{bl}| |\mathbf{E}_1| (\mathbf{R}_a'' \cos \beta + \mathbf{X}_q'' \sin \beta) - |\mathbf{V}_{bl}|^2 \left(\mathbf{R}_a'' - \frac{\sin 2\beta}{2} (\mathbf{X}_d'' - \mathbf{X}_q'') \right)}{\mathbf{R}_a''^2 + \mathbf{X}_d'' \mathbf{X}_q''} \quad (11)$$

The modified new power-angle equation can be stated as in equation no (12), if it is assumed that X_d'' is equal to X_q'' .

$$P = \frac{|V_{bl}| |E| (R_a'' \cos \beta + X_q'' \sin \beta) - |V_{bl}|^2 R_a''}{R_a''^2 + X_d''^2} \quad (12)$$

5. TRANSIENT STABILITY STUDY BASED ON THE EQUAL-AREA CRITERION

During a steady state condition in the given system, neither R_{SFCL} nor R_f exists. In this case, the value of R_a in (3) is small when compared to that of X_d' in (4). If it is assumed that R_a' is negligible, then the power-angle equation in (12) is subject to (13). In case that a fault occurs, the SFCL starts to operate with R_{SFCL} , and R_f becomes a nonzero value. Therefore, the value of R_a cannot be neglected under this condition. Therefore, the power-angle equation in (11) or (12) is now used. The factors E and δ in (11) or (12) can be calculated with the given conditions. Then, the fault current I_{fault} flowing to the ground is approximately computed by (14) during the fault applied to the infinite bus in Figure 4. Neither R_{SFCL} nor R_{f1} exists at the time of steady-state situation for the specified system. The value of R_d in (3) is less than that of X_d in (4), by comparing in this matter. The power angle equation becomes converting equation no (12) to (13) if we consider, that R_a is negligible. The equivalent power-angle curve is presented in Figure 7, wherever the subscript “ss1” indicates a steady-state condition, and therefore the dashed line specifies the initial mechanical power of 1.0379 p.u. The SFCL starts to work with R_{SFCL} , and the value of R_{f1} becomes nonzero, at the time of fault creates. So, in this condition the value of R_a cannot be neglected. As a result, the power-angle equation in (11) or (12) is currently used. The associated factors E_1 and β in (11) or (12) will be calculated with the given conditions. So as per the Figure 5, as indicated the fault current I_{fault} is flowing to the ground is almost calculated by (14) at the time of fault applied to the infinite bus

$$P_{ss1} = \frac{|E_1| |V_{bl}|}{X_d} \sin \beta \quad (13)$$

$$I_{fault} \gg \frac{(V_{bl} \angle 0^\circ)}{R_{f1}} = |I_{fault}| \angle 0^\circ = |I_{a1, fault}| \angle 0^\circ \quad (14)$$

During a fault, $|V_{bl}| \sin \beta$ and $|V_{bl}| \cos \beta$ are so small that they are also assumed to be negligible. Then, from the inspection of the phasor diagram of Figure 5(b), the voltage E_1 and its angle $(\beta + \alpha)$ are approximated by (15) and (16)), respectively,

$$\begin{aligned} |E_1| \gg X_d'' |I_{a1}| \sin(\beta + \alpha) + R_a'' |I_{a1}| \cos(\beta + \alpha) \\ 0 \gg X_q'' |I_{a1}| \cos(\beta + \alpha) - R_a'' |I_{a1}| \sin(\beta + \alpha) \end{aligned} \quad (15)$$

$$(\beta + \alpha) \gg \tan^{-1} \left(\frac{X_q''}{R_a''} \right) \quad (16)$$

The extreme values of P_{max} within the power angle curves are similar to all R_{SFCL} values. However, the value of R_{SFCL} is decreased when the corresponding power angle β with respect to P_{max} will increase.

$$f_1 = -P_{ml} (\beta_c - \beta_0) + \int_{\beta_0}^{\beta_c} P_{SFCL} d\beta + \int_{\beta_c}^{\beta_{max}} P_{ss1} d\beta - P_{ml} (\beta_{max} - \beta_c) = \int_{\beta_0}^{\beta_c} P_{SFCL} d\beta + \int_{\beta_c}^{\beta_{max}} P_{ss1} d\beta - P_{ml} (\beta_{max} - \beta_0) \quad (17)$$

Applying the equal-area criterion to the power-angle curve gives the critical clearing angle δ_c , which is the boundary point to make the system remain stable. In other words, the equal-area criterion use the function f in (17) to find the value of δ_c , which makes the value of f become zero To inspecting the system stability, the equal-area criterion use to operate the function f in (17) to find the value of β_c , that makes the value of f_1 become zero Figure 6 shows the variation of δ_c corresponding to various R_{SFCL} values (from 0 to 5 p.u.) of the SFCL.

$$t_{cl} = \sqrt{\frac{2H_i(\beta_c - \beta_0)}{\pi f I P_{ml}}} \tag{18}$$

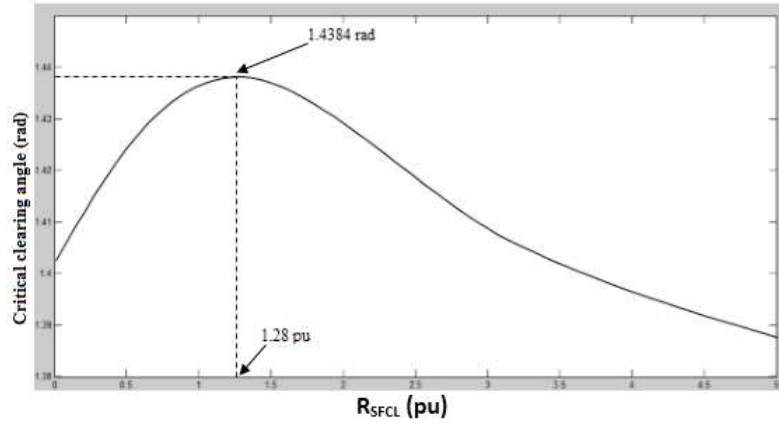


Figure 6. Variation of the critical clearing angle corresponding to R_{SFCL}

The maximum value of β_c in Figure 6 is 1.4384 rad, and the corresponding value of R_{SFCL} is 1.28 p.u. This means that R_{SFCL} of 1.28 p.u. at maximum can be optimally selected, when the SFCL is connected to this power system for protection against a fault. When power transfer during a fault is zero, (18) can also calculate the critical clearing time t_{cl} . As shown in Figure 4, the generator operates with β_0 of 0.6973 rad initially.

6. SIMULATION RESULTS

Initially, a MATLAB simulation for the system shown in Figure 7 evaluates the damping performance of the resistive SFCL. This system consists of a voltage source, $V_{s1}(t)$ of 220 V, a joint resistance R_{js} , a resistive SFCL, a fault controller with $R_f(t)$ and a resistive load with R_{L1} of 0.733 Ω . The resistive SFCL is made by a combination of three units in Figure 8 for its simulation can model this system.

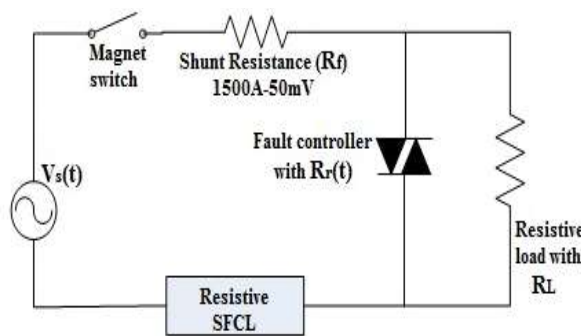


Figure 7. A 220-V/300 scale simulation test scheme circuit diagram

Then, by the finite-difference method (FDM) [18] in (19), the R_t is defined in expression (23), where it is useful to simulate the currents flowing through the circuit

$$i_t[n_t] = \left(R_t + \frac{L_t}{\Delta t} \right)^{-1} \times \left(\frac{L_t}{\Delta t} \times i_t[n_t - 1] + v_t \right) \tag{19}$$

$$= \mathbf{L} \begin{bmatrix} \mathbf{L}'_1 + \mathbf{L}'_2 + \mathbf{L}'_3 & 0 & 0 & 0 & 0 \\ 0 & 0 & 0 & 0 & 0 \\ 0 & 0 & 0 & 0 & 0 \\ 0 & 0 & 0 & 0 & 0 \\ 0 & 0 & 0 & 0 & 0 \end{bmatrix} \quad (20)$$

$$\mathbf{i}_t = [\mathbf{i}_s(t) \quad \mathbf{i}_1(t) \quad \mathbf{i}_2(t) \quad \mathbf{i}_3(t) \quad \mathbf{i}_f(t)]^T \quad (21)$$

$$\mathbf{v}_t = [\mathbf{V}_{s1}(t) \quad 0 \quad 0 \quad 0 \quad 0]^T \quad (22)$$

$$\mathbf{R}_t = \begin{bmatrix} \mathbf{R}_j + \mathbf{R}_{ic}(t) + \mathbf{R}_{2c}(t) + \mathbf{R}_{3c}(t) + \mathbf{R}_L & -\mathbf{R}_{ic}(t) & -\mathbf{R}_{2c}(t) & -\mathbf{R}_{3c}(t) & -\mathbf{R}_L \\ -\mathbf{R}_{ic}(t) & \mathbf{R}_{ic}(t) + \mathbf{R}_{is}(t) & 0 & 0 & 0 \\ -\mathbf{R}_{2c}(t) & 0 & \mathbf{R}_{2c}(t) + \mathbf{R}_{2s}(t) & 0 & 0 \\ -\mathbf{R}_{3c}(t) & 0 & 0 & \mathbf{R}_{3c}(t) + \mathbf{R}_{3s}(t) & 0 \\ -\mathbf{R}_L & 0 & 0 & 0 & \mathbf{R}_L(t) + \mathbf{R}_f(t) \end{bmatrix} \quad (23)$$

where n is the number of step and Δ tis the time length of the FDM step. The associated inductor matrix (L), current vector \bar{i}_t , voltage vector \bar{v}_t , and resistor matrix \bar{R}_t are given in (20)-(23), respectively. In comparisonto the case while not the SFCL, the SFCL improves the damping performance to decrease the level of I_s vey successfully throughout a fault.

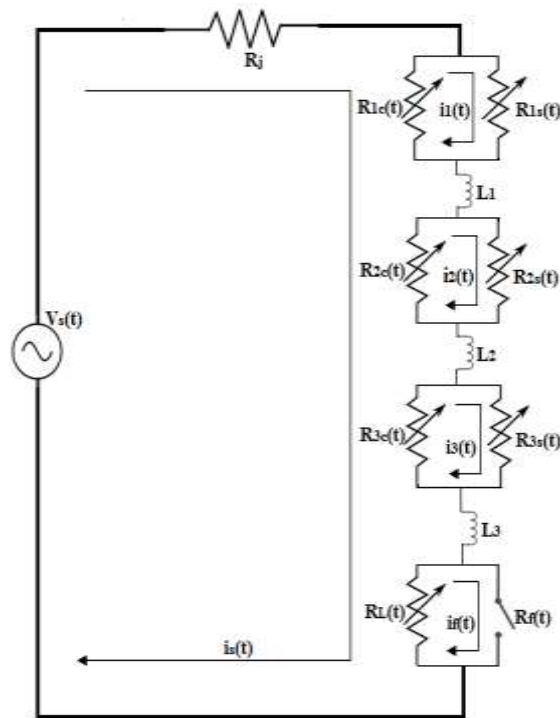


Figure 8. Equivalent circuit of the test system

7. SMIB SYSTEM

The MATLAB based simulation model on the SMIB system as represented in Figure 4, is the estimation of the damping performance of the SFCL with an optimal value of R_{SFCL} . Therefore, here the corresponding critical clearing angle δ_c to the optimal value of R_{SFCL} is 1.4384 rad, as primarily it is mentioned that the R_{SFCL} value of 1.28 p.u. is optimally selected by the transient stability analysis based on the equal-area criterion. Here the respective Power (P) vs. angle (δ) curve and swing curves for that system are shown in Figure 9-11 respectively.

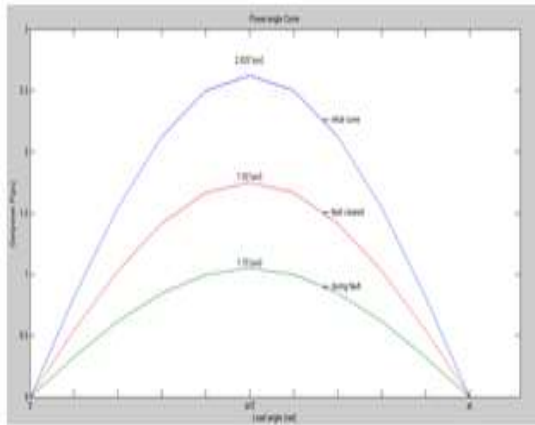


Figure 9. Power (P) vs angle (δ) curve

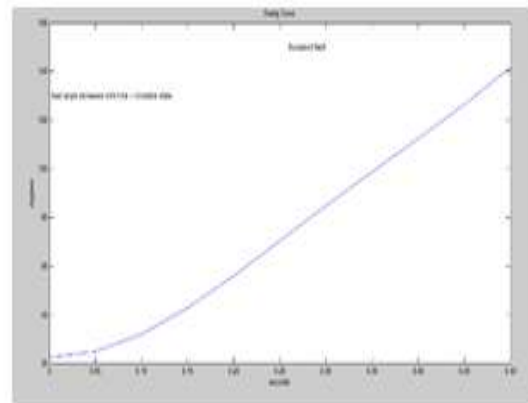


Figure 10. Swing curve for sustained fault

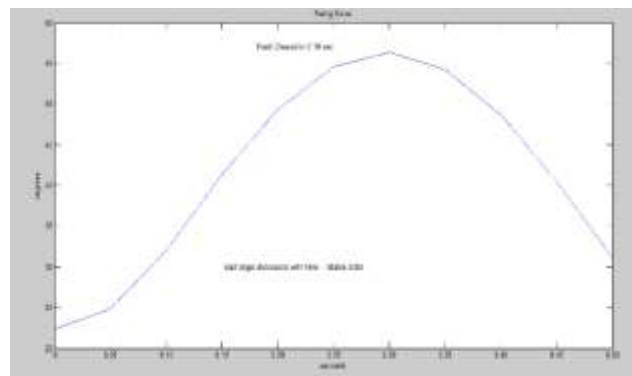


Figure 11. Swing curve when fault is cleared in 0.10 sec

In addition, here the respective time vs. voltage and current waveforms are shown in Figure 12- 19 based on to run the Simulink circuit indicated as Figure 1 for different mode of operation for applying the gate signal in SFCL circuit.

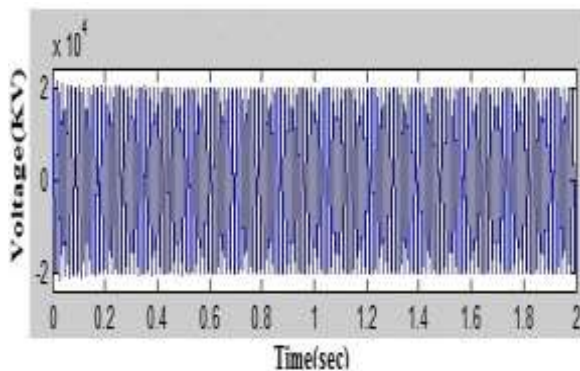


Figure 12. Phase a to ground voltage vs. time response for three Series RLC load

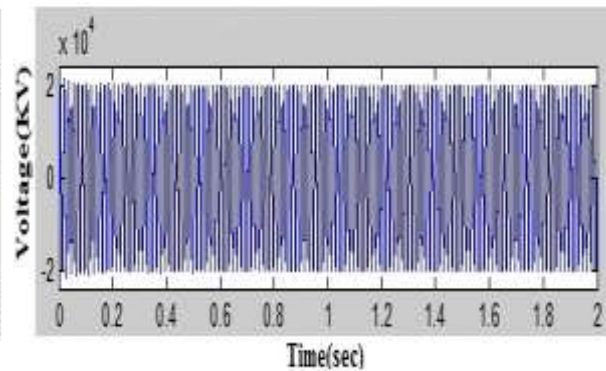


Figure 13. Source phase voltage vs. time response for distributed parameters

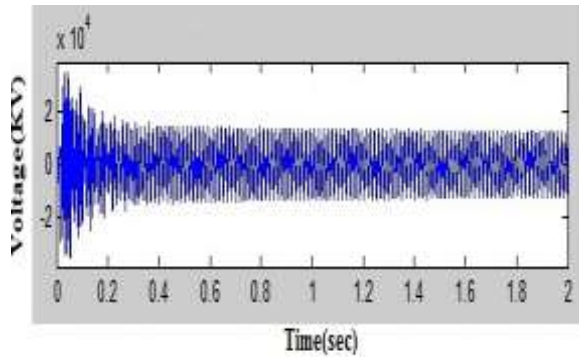


Figure 14. Phase a to ground voltage vs. time response for Three-phase Transformer

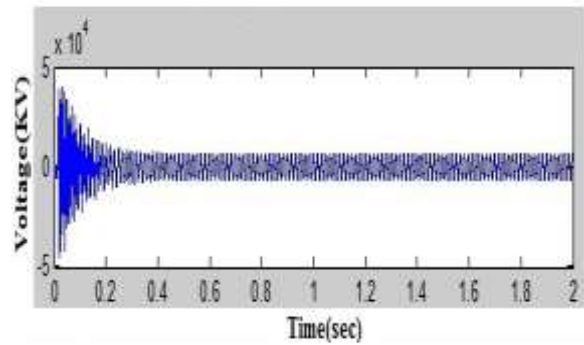


Figure 15. Phase b to ground voltage VS time response for Three-phase Transformer

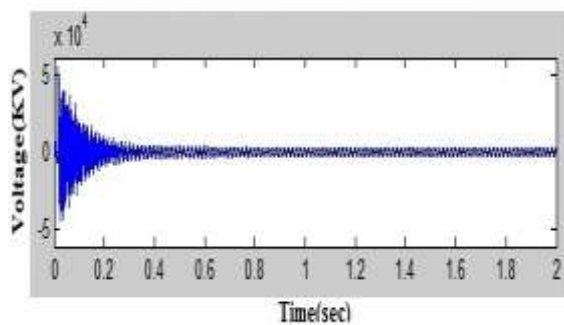


Figure 16. Phase C to ground voltage vs. time response for Three-phase Transformer

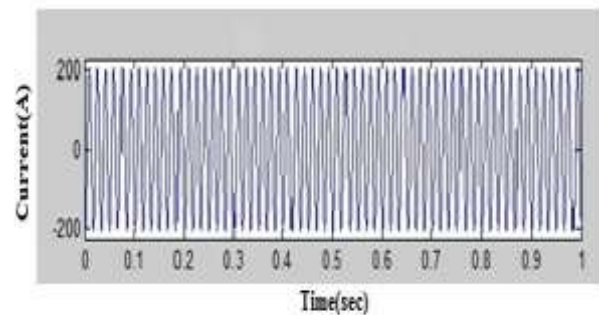


Figure 17. Phase a to ground current vs. time response for three phase series RLC load

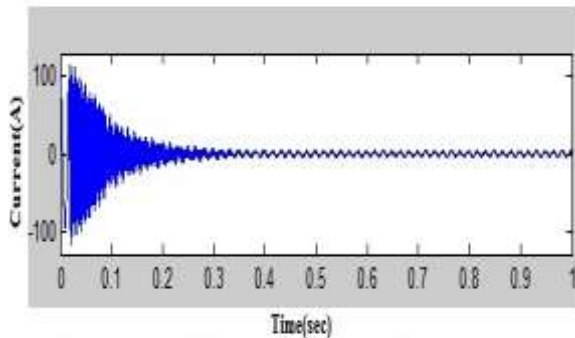


Figure 18. Phase B to ground current vs. time response for three phase series RLC load

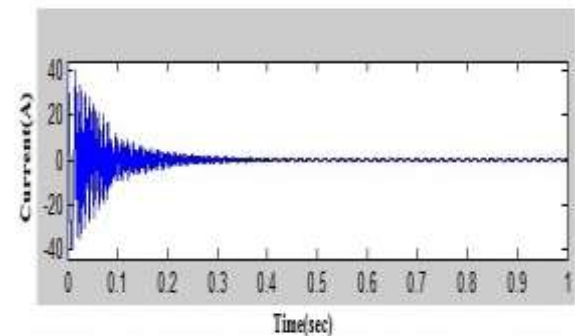


Figure 19. Phase C to ground current vs. time response for three-phase Transformer

8. CONCLUSION

This paper planned the study to determine the optimal resistive value (R_{SFCL}) of a resistive SFCL by analyzing the transient stability based on the equal-area criterion. The damping performances of the SFCL during a fault were evaluated by case studies on simulation results. It was shown from the results that the resistive SFCL with the optimally selected R_{SFCL} is very effective to reduce the level of short-circuit current dramatically. Therefore, the reliability and stability of the power system can be improved by the application of the SFCL. On the other way, existing protecting devices, like as a recloser, might not be operated properly once the fault current level is extremely low by damping that the SFCL will give. With many case studies, these issues are being investigated.

REFERENCES

- [1] Alok Kumar Shrivastav, Pradip Kumar Sadhu, Ankur Ganguly, Nitai Pal, "A Novel Transient Fault Current limiter based on three phase Thyristor Bridge for Y-yg transformer", *International Journal of Power Electronics and Drives System*, Vol. 6(4), December 2015, PP. 747 – 758.
- [2] S. Sugimoto, J. Kida, H. Arita, C. Fakui, and T. Yamagiwa, "Principle and characteristics of a fault current limiter with series compensation", *IEEE Trans. Power Delivery*, vol. 11, no. 2, pp. 842–847, Apr. 1996.
- [3] T. Jamasb, W.J. Nuttall, and M. G. Pollitt, *Future Electricity Technologies and Systems*. Cambridge: Cambridge Univ. Press, 2006, pp. 83–97, 235–246.
- [4] B.C. Sung, D.K. Park, J.W. Park, and T.K. Ko, "Study on a series resistive SFCL to improve power system transient stability: Modelling ,simulation and experimental verification", *IEEE Trans. Industrial Electron.*, vol. 56, no. 7, pp. 2412–2419, Jul. 2009.
- [5] Pradip Kumar Sadhu, Saumen Dhara, Alok Kumar Shrivastav, Debabrata Roy, "Superconducting Fault Current Limiters for Micro Grid Application", *International Journal of Mechatronics and Computer Technology*, Vol. 5(16), Jul. 2015, PP. 2246 – 2257
- [6] Alok Kumar Shrivastav, Pradip Kumar Sadhu, Ankur Ganguly, "Comparative Stability and Harmonic Analysis Based On Transient Current Limiter in Distribution System", Proceeding of IEEE (EDS) Kolkata Chapter Sponsored 4thInternational Conference on Computing, Communication and Sensor Network, December 2015, ISBN: 81-85824-46-0, PP 108-114.
- [7] M. Noe and M. Strurer, "High-temperature superconductor fault current limiters: Concepts, applications, and development status", *Supercond. Sci. Technol.*, vol. 20, no. 3, pp. R15–R29, Mar. 2007.
- [8] H. Hatta, S. Muroya, T. Nitta, Y. Shirai, and M. Taguchi, "Experimental study on limiting operation of superconducting fault current limiter in double circuit transmission line model system", *IEEE Trans. Appl. Supercond.*, vol. 12, no. 1, pp. 812–815, Mar. 2002.
- [9] L. Ye, L.Z. Lin, and K.P. Juengst, "Application studies of superconducting fault current limiters in electric power systems", *IEEE Trans. Appl. Superconductor*, vol. 12, no. 1, pp. 900–903, Mar. 2002.
- [10] Y. Shirai, M. Taguchi, M. Shiotsu, H. Hatta, and T. Nitta, "Simulations study on operating characteristics of superconductor fault current limiter in one-machine infinite bus power system", *IEEE Trans. Appl. Super-cond.*, vol. 13, no. 2, pp. 1822–1827, Jun. 2003.
- [11] T. Nomura, M. Yamaguchi, S. Fukui, K. Yokoyama, T. Satoh, and K. Usui, "Single DC reactor type fault current limiter for 6.6 kV power system", *IEEE Trans. Appl. Superconductor*, vol. 11, no. 1, pp. 2090–2093, March. 2001.
- [12] H. Yamaguchi, T. Kataoka, K. Yaguchi, S. Fujita, K. Yoshikawa, and K. Kaiho, "Characteristic analysis of transformer type superconducting fault current limiter", *IEEE Trans. Appl. Supercond.*, vol. 14, no. 2, pp. 815–818, Jun. 2004.
- [13] Y. Goto, K. Yukita, H. Yamada, K. Ichianagi, Y. Yokomizu, and T. Matsumura, "A study on power system transient stability due to in-troduction of superconducting fault current limiters", in Proc. Int. Conf. Powercon, 2000, pp. 275–280.
- [14] K. Maki, S. Repo, and P. Jarventausta, "Effect of wind power based distributed generation on protection of distribution network", in *IEEE Developments in Power System Protection*, Dec. 2004, vol. 1, pp. 327–330.

BIOGRAPHIES OF AUTHORS



Saumen Dhara received his B.E Degree in Electrical Engineering from Burdwan University, West Bengal, India in 2002 and M.E in 2007 from Jadavpur University, West Bengal, India. He has total thirteen years of experience in the field of teaching. Presently he is working as a Assistant Professor in the Department of Electrical Engineering, Saroj Mohan Institute of Technology, Guptipara, Hooghly-712512, West Bengal, India. He is presently pursuing Ph.D. programme at the Department of Electrical Engineering, Indian School of Mines, Dhanbad-826004, India. His research area of interests includes Power system, Power electronics, Investigation and analysis of faults in power system for power quality improvement.



Alok Kumar Shrivastav received his B.Tech degree in Electrical & Electronics Engineering from West Bengal University of Technology, West Bengal, India, in 2009, the M.Tech degree in Electrical Engineering from NIT Durgapur, West Bengal, India, in 2013, and presently pursuing Ph.D. programme at the Department of Electrical Engineering, Indian School of Mines, Dhanbad-826004, India. He has several publications in International and National journals and has also presented several papers in International and National conferences. He is reviewer of journals like IEI, Springer etc. He is presently Assistant Professor, Batanagar Institute of Engineering, Management and Science, Maheshtala, Kolkata. His special field of interest is in power quality in distribution system, power flow monitoring and stability analysis.



Pradip Kumar Sadhu received his Bachelor, Post-Graduate and Ph.D. (Engineering) degrees in 1997, 1999 and 2002 respectively in Electrical Engg. From Jadavpur University, West Bengal, India. Currently, he is working as a Professor in Electrical Engineering Department of Indian School of Mines, Dhanbad, India. He has total experience of 18 years in teaching and industry. He has four Patents. He has several journal and conference publications in national and international level. He is principal investigator of few Govt. funded projects. He has guided a large no. of doctoral candidates and M. Tech students. His current areas of interest are power electronics applications, application of high frequency converter, energy efficient devices, energy efficient drives, computer aided power system analysis, condition monitoring, and lighting and communication systems for underground coal mines.



Ankur Ganguly received his B.E. degree in Electrical & Electronics Engineering from Mangalore University, Karnataka, India, in 2000, the M.Tech. degree in Biomedical Engineering from MAHE, Manipal, Karnataka, India, in 2002, and the Ph.D. degree in Engineering from Jadavpur University, Kolkata, India, in 2011. He is presently Professor and Principal, Batanagar Institute of Engineering, Management and Science, Maheshtala, Kolkata. His research interests include biomedical signal processing, chaos theory, heart rate variability. At present, he is engaged in Non Linear applications and chaos theory in HRV and electrical machines.